Cross-Platform Identification and Validation of Uveal Melanoma Vitreous Protein Biomarkers

Gabriel Velez,[1,2] Julian Wolf,[1,2] Antoine Dufour,[3] Prithvi Mruthyunjaya,[2] and Vinit B. Mahajan[1,2,4]

[1]Molecular Surgery Laboratory, Stanford University, Palo Alto, California, United States
[2]Department of Ophthalmology, Byers Eye Institute, Stanford University, Palo Alto, California, United States
[3]Department of Physiology and Pharmacology, Cumming School of Medicine, University of Calgary, Calgary, AB, Canada
[4]Veterans Affairs Palo Alto Health Care System, Palo Alto, California, United States

Correspondence: Vinit B. Mahajan and Prithvi Mruthyunjaya, Byers Eye Institute, Department of Ophthalmology, Stanford University, Palo Alto, CA 94304, USA; vinit.mahajan@stanford.edu and prithvi9@stanford.edu.

Received: June 29, 2023
Accepted: October 20, 2023
Published: November 13, 2023

Citation: Velez G, Wolf J, Dufour A, Mruthyunjaya P, Mahajan VB. Cross-platform identification and validation of uveal melanoma vitreous protein biomarkers. *Invest Ophthalmol Vis Sci.* 2023;64(14):14. https://doi.org/10.1167/iovs.64.14.14

Purpose. The purpose of this study was to profile protein expression liquid vitreous biopsies from patients with uveal melanoma (UM) using mass spectrometry to identify prognostic biomarkers, signaling pathways, and therapeutic targets.

Methods. Vitreous biopsies were collected from two cohorts in a pilot study: comparative control eyes with epiretinal membranes (ERM; $n = 3$) and test eyes with UM ($n = 8$). Samples were analyzed using liquid chromatography-tandem mass spectrometry (LC-MS/MS). Identified proteins were compared to data from a targeted multiplex ELISA proteomics platform.

Results. A total of 69 significantly elevated proteins were detected in the UM vitreous, including LYVE-1. LC-MS/MS identified 62 significantly upregulated proteins in UM vitreous that were not previously identified by ELISA. Analysis of differential protein expression by tumor molecular classification (gene expression profiling [GEP] and preferentially expressed antigen in melanoma [PRAME]) further identified proteins that correlated with these classifications. Patients with high-risk GEP tumors displayed elevated vitreous expression of HGFR (fold-change [FC] = 2.66E + 03, P value = 0.003) and PYGL (FC = 1.02E + 04, P = 1.72E-08). Patients with PRAME positive tumors displayed elevated vitreous expression of ENPP-2 (FC = 3.21, $P = 0.04$), NEO1 (FC = 2.65E + 03, $P = 0.002$), and LRP1 (FC = 5.59E + 02, P value = 0.01). IGF regulatory effectors were highly represented (P value = 1.74E-16). Cross-platform analysis validated seven proteins identified by ELISA and LC-MS/MS.

Conclusions. Proteomic analysis of liquid biopsies may provide prognostic information supporting gene expression of tumor biopsies. The use of multiple protein detection platforms in the same patient samples increases the sensitivity of candidate biomarker detection and allows for precise characterization of the vitreous proteome.

Keywords: uveal melanoma (UM), proteomics, vitreous humor

Uveal melanoma (UM) is the most common primary intraocular tumor in adults, affecting approximately 5 to 11 individuals per million per year.[1,2] Approximately 50% of patients with UM develop metastatic disease, most commonly in the liver. Once confirmed to have metastatic disease, patients may be treated with liver directed therapies, systemic chemotherapy, or immunotherapies, including checkpoint inhibition, however, survival prognosis remains poor.[3] It is suspected that micro-metastatic disease may develop up to 1 to 5 years prior to detection and conservative treatment of the primary tumor.[4] Despite this, methods for clinically detecting micro-metastatic disease remain limited.[5] Thus, it is critical to identify patients at risk for micro-metastatic disease, so that adjuvant systemic therapy can be used judiciously to delay or prevent the development of clinically significant macro-metastatic disease.[5,6]

To determine patients at higher risk for developing metastatic disease, clinical or histopathologic risk factors are considered,[7,8] but advances in genetic testing of primary tumors have enhanced the prognostic accuracy.[9] The Collaborative Ocular Oncology Group prospectively validated a gene expression profiling platform (GEP; Decision Dx-UM, Castle Biosciences, Fraunwald, TX, USA) using a quantitative PCR (qPCR)-based assay as the most accurate method to predict risk of UM metastasis and is a stronger predictor than either chromosomal status or clinical features alone.[10] Two major subclasses were identified based on GEP analysis which correlate with low (i.e. class 1) and high (i.e. class 2) risk of metastatasis.[11] Recently, another prognostic biomarker, preferentially expressed antigen in melanoma (PRAME; Decision Dx-PRAME, Castle Biosciences, Fraunwald, TX, USA), appears to be a risk modifier associated with increased metastatic risk, and the combination of GEP and PRAME together can provide prognostic accuracy superior to TNM staging.[12] Whereas GEP and PRAME testing are beneficial for assessing mortality risk, they require

invasive surgical sampling of the primary uveal tumor. Although tumor biopsies have become the standard of care, they carry the risk of retinal detachment and other vision-threatening side effects such as hemorrhage along with sampling bias (e.g. in the setting of tumor heterogeneity or inability to obtain an adequate sample from a small tumor). Moreover, they are neither amenable nor are current clinical tests validated for repeat testing after definitive therapy (e.g. post-enucleation or radiation therapy).[13–16]

Proteomic analysis is becoming an attractive and powerful tool for characterizing the molecular profiles of diseased tissues.[17] Ocular liquid biopsies (e.g. anterior chamber taps and diagnostic vitrectomies) may serve as a less invasive alternative to primary UM tumor biopsies for monitoring disease progression and response to therapy.[18] Additionally, liquid biopsies lend themselves to repeat testing, allowing for prospective surveillance of patients' metastatic risk.[19] Validation of proteomic biomarkers on different platforms strengthens the potential value of diagnostic vitreous biomarkers for early screening and therapeutic monitoring. Furthermore, protein signatures could detect molecular changes in the primary tumor, uncover diagnostic and prognostic biomarkers, and point to potential candidates for drug repositioning and adjuvant therapy.[20,21]

Previously, we performed quantitative proteomic analysis (i.e. multiplex ELISA) on vitreous humor from patients with UM and identified several protein biomarkers (e.g. HGFR/c-Met, autotaxin, etc.) that correlated with the molecular profiles of the primary tumor.[22] However, analysis was limited to 1000 preselected proteins and did not provide a comprehensive survey of the vitreous proteome. In the current study, we obtained a more global view of the UM vitreous proteome using liquid chromatography-tandem mass spectrometry (LC-MS/MS).

Methods

Study Approval

The study was approved by the Stanford University Institutional Review Board and adhered to the tenets set forth in the Declaration of Helsinki. Subjects underwent eye examinations that included slit-lamp examination, dilated retinal bio-microscopy, and indirect ophthalmoscopy by an ocular oncologist (author P.M.). Data were collected and analyzed from November 2018 to April 2023.

Vitreous Sample Collection

Liquid vitreous biopsies were collected from two groups: eyes from control subjects ($n = 3$) with epiretinal membranes (ERMs), and eyes from test subjects ($n = 8$) with UM. In eyes undergoing I-125 plaque brachytherapy for UM treatment or control eyes with ERM, a standard 3 port pars plana vitrectomy setup was used with a single-step transconjunctival 27-gauge trocar cannular system (Alcon Laboratories Inc, Fort Worth, TX, USA). Undiluted 0.5 to 1.0 mL sample of the vitreous was manually aspirated into a 5 mL syringe prior to obtain a primary tumor biopsy using a vitrectomy cutter approach.[23] For UM eyes undergoing enucleation, after the globe was removed, trans scleral fine-needle aspiration (FNA) biopsy was performed to obtain primary tumor biopsy, and then an 18-gauge needle was inserted through the pars plana in the quadrant opposite the bulk of the tumor and 1 to 2 mL of vitreous fluid was removed. Vitreous samples were immediately centrifuged in the operating room at 15,000 × g for 5 minutes at room temperature to remove impurities and then finally stored at −80°C, as previously described.[24]

Primary Tumor Analysis

The GEP profile of the tumor samples was determined as previously described.[12,25] Briefly, an FNA or vitrectomy assisted biopsy of the tumor was performed at the time of I-125 plaque brachytherapy or at the time of enucleation.[16,23] Tumor samples underwent RNA extraction followed by reverse transcription to generate cDNA for analysis by real-time quantitative PCR (Decision Dx-UM; Castle Biosciences).[12,25] The PRAME status of the tumor samples was determined by measuring *PRAME* mRNA expression on an Illumina HT-12v4 chip using probe ILMN_1700031 as described previously (Decision Dx-UM PRAME, Castle Biosciences).[26]

Protein Extraction, Digestion, and Peptide Desalting

A shotgun proteomics screen was performed to identify biomarkers not sampled in our multiplex ELISA. Vitreous humor samples were albumin-depleted using affinity chromatography. Briefly, 100 µL of undiluted vitreous was loaded onto midi columns containing Top14 Abundant Protein Depletion resin (Thermo Scientific) and incubated at room temperature for 10 minutes with gentle mixing. Columns were then placed in 15 mL conical tubes and centrifuged at 1000 × g for 2 minutes and the filtrate discarded. Unbound proteins were eluted in 10 mM PBS (pH 7.4) and 0.02% sodium azide and protein concentration was determined by Bradford assay. A total of 5 µg of protein per sample was diluted in 50 mM ammonium bicarbonate to a final volume of 1 mL and reduced by addition of 10 mM DTT followed by incubation at 55°C for 30 minutes. Alkylation was performed by adding 1 M acrylamide for a final concentration of 30 mM and incubating at room temperature for 30 minutes. Trypsin (0.5 µg) was then added to each tube and samples were digested overnight at 37°C. The reaction was quenched by adding 50% formic acid to a final concentration of 2%. Digested peptides were desalted using C18 stop-and-go extraction (STAGE) tips. Briefly, for each sample, a C18 STAGE tip was equilibrated with 0.1% trifluoroacetic acid (TFA) followed by 50% acetonitrile (ACN). Samples were loaded onto the tips and desalted with 50% ACN. Peptides were eluted with 0.1% formic acid in 50% ACN and lyophilized in a SpeedVac to dryness.

Liquid Chromatography-Tandem Mass Spectrometry

Peptide pools were reconstituted in 15 µL of 2% ACN and 0.1% formic acid solution. A total of 3 µL of each sample was injected into an in-house packed C18 reverse phase analytical column (15 cm in length). Ultra-performance liquid chromatography (UPLC) was performed on a Waters M-Class at a flow rate of 0.45 µL/min using a linear gradient from 4% to 40% Mobile phase B (0.2% formic acid, 99.8% ACN). Mobile phase A consisted of 0.2% formic acid. Mass spectrometry was performed on an Orbitrap fusion set to acquire data in a dependent fashion using the top-speed functionality.

Investigative Ophthalmology & Visual Science

Fragmentation was performed on the most intense multiply charged precursor ions using collision induced dissociation (CID). The mass spectrometry data were analyzed using Preview and Byonic software (ProteinMetrics) to identify peptides and infer proteins using the Uniprot homo sapiens annotated databases files including isoforms, concatenated with common contaminant proteins. Analysis was performed at 12 ppm mass tolerances for precursor ions, with 0.4 Da windows for fragment ions; only peptides with fully tryptic cleavages were tolerated, with up to 2 missed cleavage sites. Data were validated using the standard reverse-decoy techniques at a 1% false discovery rate. The mass spectrometry proteomics data were deposited to the ProteomeXchange Consortium via the PRIDE partner repository with the dataset identifier PXD043403 and 10.6019/PXD043403.

Statistical and Bioinformatic Analysis

Results from the separate datasets were saved in Excel as .txt format and were uploaded into the Partek Genomics Suite 6.5 software package. The data was normalized to log base 2 and compared using 1-way ANOVA analysis. All proteins with nonsignificant ($P > 0.05$) changes were eliminated from the table. The significant values were mapped using the "cluster based on significant genes" visualization function with the standardization option chosen. Principal component analysis (PCA) was performed with Qlucore Omics Explorer version 3.8. Gene ontology enrichment and pathway analysis was performed using g:Profiler and Reactome, respectively, using default parameters.[27,28]

Results

Functional Characterization of the UM Vitreous Proteome

A cohort of eight patients were diagnosed with UM and used for the analysis (see the Table). Three cases of patients with idiopathic epiretinal membrane were used for comparative controls. The average patient age was 53.9 ± 16.3 years; 75% were men. Mean tumor thickness was 6.6 mm and largest basal diameter was 14.0 mm. The eighth edition American Joint Commission on Cancer (AJCC) classification was stage I ($n = 1$), stage IIA ($n = 3$), stage IIB ($n = 3$), and stage IIIA ($n = 1$).[29,30] UM tumor biopsies revealed GEP class 1 in 5 patients and class 2 in 3 patients. Fifty percent of the patients were PRAME positive.[10,31,32] Half the patients received plaque brachytherapy, with the other half undergoing enucleation. Vitreous specimens were safely obtained without complication. Uveal melanoma and control vitreous samples were albumin-depleted and underwent trypsinization followed by multidimensional liquid chromatography before analysis by tandem mass spectrometry (Supplementary Table S1). We identified 380 ± 122 (mean ± SD) individual proteins (6600 ± 2469 spectra with 4218 ± 1309 unique peptides) in UM vitreous and 253 ± 88 individual proteins (2844 ± 2405 spectra with 2022 ± 1222 unique peptides) in control vitreous (Fig. 1A). The most abundant proteins identified in UM and control vitreous, other than albumin, were complement C3 (C3), hemopexin (HPX), ceruloplasmin (CP), and vitamin D-binding protein (VTDB; Fig. 1B).

Proteins with a mean spectral count greater than two were subsequently analyzed using gene ontology enrichment analysis and were classified by their respective cellular compartment and molecular function. When categorized by cellular compartment, most vitreous proteins (90%; 3.08E-167) were either extracellular or localized to collagen-containing extracellular complexes (Fig. 1C). A significant fraction of proteins identified in UM vitreous were involved in endopeptidase inhibition (14%; $P = 3.56E-35$) and glycosaminoglycan activity (13%; $P = 8.55E-27$; Fig. 1D).

Shotgun Proteomic Analysis Distinguishes Molecular Classes of Uveal Melanoma

Protein spectral counts were analyzed with 1-way ANOVA to identify differentially expressed proteins (DEPs) in UM vitreous. A total of 69 proteins were differentially expressed among control and UM samples (64 upregulated proteins and 5 downregulated proteins; $P < 0.05$; Fig. 2A; Supplementary Table S2). Among the upregulated proteins were carboxypeptidase 2 (CBPB2) and lymphatic vessel endothelial hyaluronic acid receptor 1 (LYVE-1; P value = 3.94E-9, fold-change = 2164; see Fig. 2A). Because primary UM tumors can be classified by GEP class or PRAME status, we sought to identify protein signatures that were associated with these molecular classifications. When comparing protein expression by PRAME status, there were 48 differentially expressed proteins (43 upregulated proteins and 5 downregulated proteins) at the $P < 0.05$ level (Fig. 2B, Supplementary Table S4). Among the upregulated proteins in PRAME positive vitreous were ectonucleotide pyrophosphatase/phosphodiesterase family member 2 (ENPP-2/autotaxin), neogenin (NEO1), and prolow-density lipoprotein receptor-related protein 1 (LRP1; see Fig. 2B). ENPP-2/autotaxin and HGFR/c-MET were identified

Table. Demographics for the UM Cohort

Case	1	2	3	4	5	6	7	8
GEP	1B	1A	2	1A	1A	2	1B	2
PRAME	Positive	Positive	Positive	Negative	Negative	Positive	Negative	Negative
AJCC stage	IIIA	IA	IIA	IIA	IIA	IIB	IIB	IIB
T stage	T3a	T1a	T2a	T2a	T2a	T4b	T3a	T3a
Eye	OS	OS	OS	OD	OD	OS	OS	OS
Age (years)	67	30	80	47	57	57	35	58
Sex	M	F	M	M	M	M	F	M
Largest basal diameter (mm)	16	6	12.7	11.5	11	21.8	15.6	15.6
Minor diameter (mm)	13.7	7	11.2	11.8	9	16.7	15.9	14.5
Tumor height (mm)	5.8	5.8	4.8	7.5	3.9	12.8	7.3	7.3

GEP class, gene expression profile; PRAME, preferentially expressed antigen in melanoma; AJCC, American Joint Committee on Cancer; T stage, tumor stage.

Investigative Ophthalmology & Visual Science

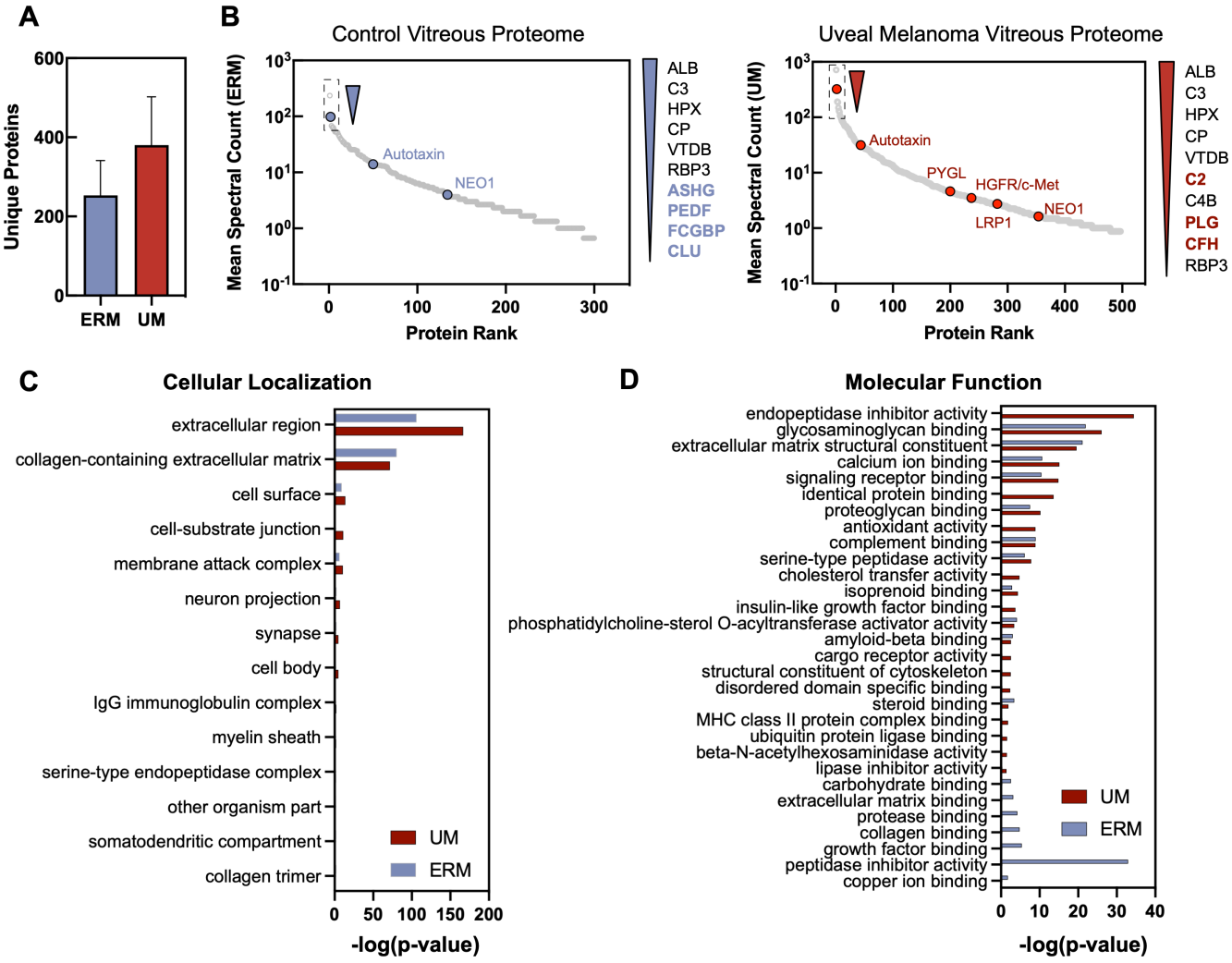

Figure 1. Functional characterization of the UM vitreous. (**A**) Number of unique proteins identified in ERM and UM vitreous. (**B**) Relative abundance (mean spectral counts) of human vitreous proteins with several illustrative proteins highlighted in blue (ERM, *left*) and red (UM, *right*). Gene ontology analysis of the proteins identified in ERM and UM vitreous. Proteins are grouped into subcategories based on their respective (**C**) cellular localization and (**D**) molecular function.

in our previously published quantitative proteomics study on UM vitreous (i.e. multiplex ELISA) and their detection on a separate proteomic platform further validates these proteins as vitreous biomarkers for UM.[22] Protein expression was next compared between GEP class 1 and class 2 vitreous. Due to the small sample size, a dichotomous comparison was performed rather than comparison of the 3 GEP groups (i.e. class 1A, 1B, and 2). There were 53 differentially expressed proteins (43 upregulated proteins and 10 downregulated proteins) at the $P < 0.05$ level (Fig. 2C, Supplementary Table S3). Among the upregulated proteins in GEP class 2, vitreous were hepatocyte growth factor receptor (HGFR/c-MET) and liver glycogen phosphorylase (PYGL; see Fig. 2C).

The IGF1 Regulatory Effectors Are Highly Represented in UM Vitreous

To classify differentially expressed proteins in UM vitreous, we performed pathway analysis (Fig. 3A). The top represented pathways in GEP class 1 vitreous were platelet degranulation and activation, collagen degradation, and hyaluronan metabolism. The top represented pathways in GEP class 2 vitreous were metabolic processes (glycolysis, gluconeogenesis, and amino acid biosynthesis), neutrophil degranulation, and innate immune system. The top represented pathways in PRAME positive (versus PRAME negative) vitreous were complement cascade, coagulation cascade, and regulation of insulin-growth factor (IGF) by IGF-binding proteins (IGFBPs; P value = 1.74E-16; see Fig. 3A). The high representation of metabolic pathways in GEP class 2 and PRAME positive UM vitreous may be due to reprograming by the primary tumor to meet its increased metabolic demands.[33] Prior studies suggested that increased expression levels of IGF1 receptor (IGFR-1) in primary UM tumors is associated with increased risk of death from metastatic disease in patients with UM.[34] A total of 16 IGF1 regulatory effectors were differentially expressed in UM vitreous at the $P < 0.05$ level (Supplementary Table S5). These results suggest that IGF1 regulatory effectors, likely originating from the tumor, can be detected in the vitreous of patients at high risk for metastatic disease.

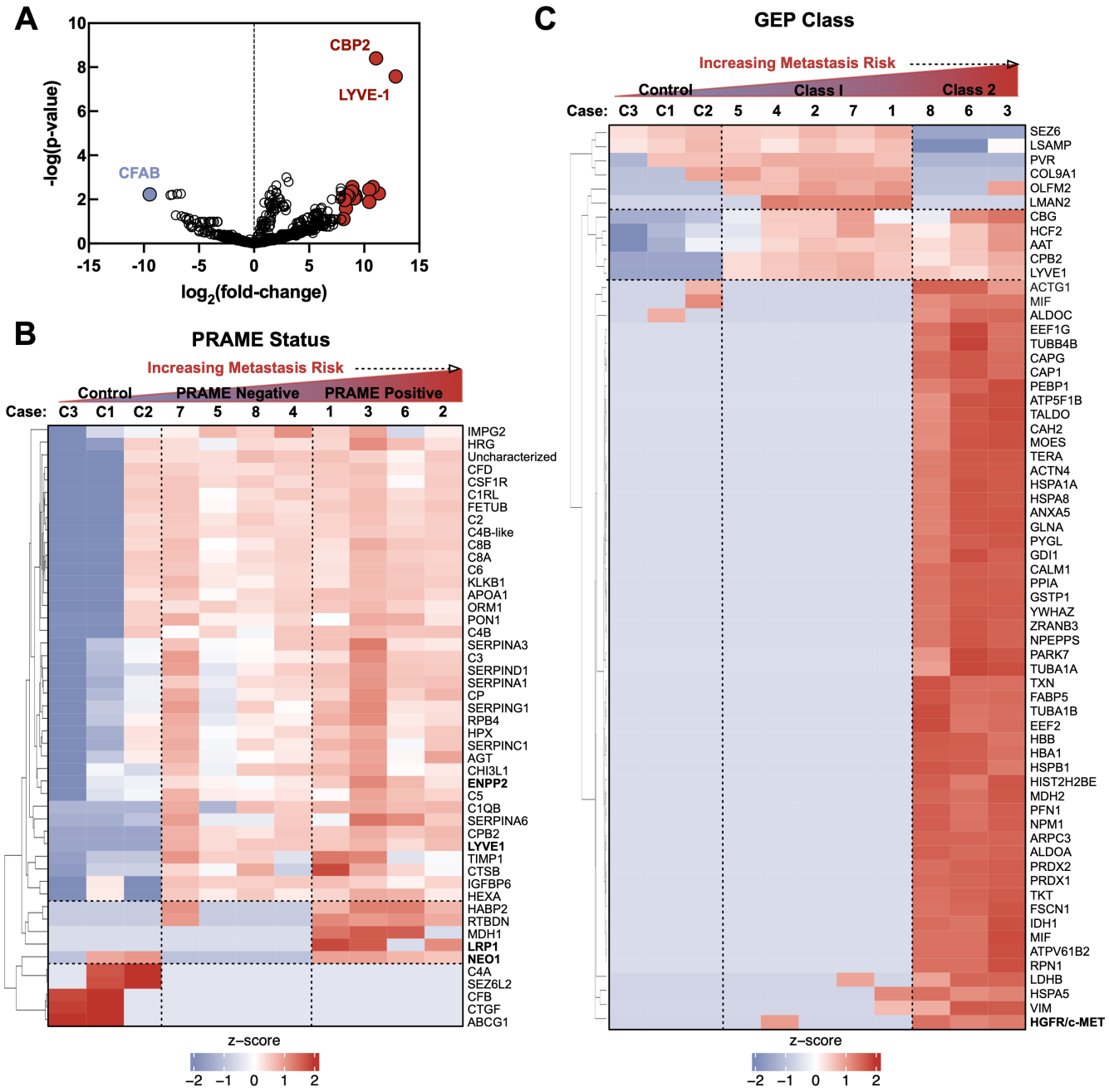

Figure 2. Shotgun proteomic signatures differentiate molecular classes of uveal melanoma. (**A**) Differentially expressed proteins (between UM and control vitreous) detected by LC-MS/MS represented as a volcano plot. The horizontal axis (x-axis) displays the log2 fold-change value (UM versus controls) and the vertical axis (y-axis) displays the noise-adjusted signal as the -log10 (*P* value). (**B**) Multi-group comparison (1-way ANOVA) followed by hierarchical heat map clustering was used to identify differentially expressed proteins based on PRAME status and GEP class. When comparing protein expression by PRAME status, there were 48 differentially expressed proteins at the $P < 0.05$ level. Results are represented as a heatmap and display protein expression levels on a logarithmic scale. *Red* indicates high expression whereas *white/blue* indicates low or no expression. (**C**) When comparing protein expression by GEP class, there were 53 differentially expressed proteins at the $P < 0.05$ level.

Cross-Platform Validation of UM Vitreous Biomarkers

We next sought to compare upregulated proteins identified by LC-MS/MS to those previously identified by multiplex ELISA in the same samples. We compared significantly upregulated proteins (compared to controls) at the $P < 0.05$ level between LC-MS/MS and multiplex ELISA. There were two commonly identified proteins among these groups (LYVE-1 and plasminogen; Fig. 3B). We next compared lists of upregulated proteins, sorted by PRAME status and GEP class (Fig. 3C). PRAME positive and PRAME negative samples exhibited similar vitreous protein expression in this comparision and only two proteins (angiotensinogen and ENPP2) were commonly detected by LC-MS/MS and multiplex ELISA. There were 2 commonly identified proteins (C163A and

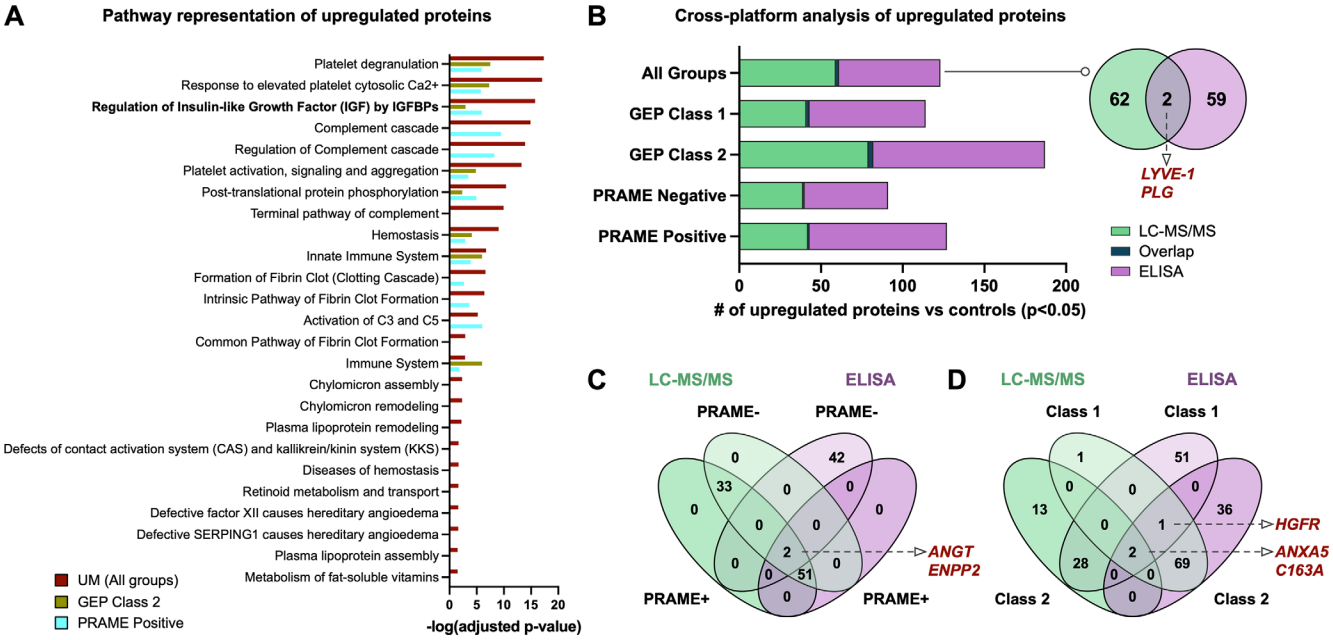

Figure 3. Cross-platform identification and validation of UM biomarkers. (**A**) Top pathways represented in UM vitreous. Pathways are ranked by their -log (*P* value) obtained from the right-tailed Fisher's Exact Test and colored by their respective subclassification: GEP class 2, *yellow*; PRAME positive, *cyan*; and all UM samples, *red*. (**B**) Comparative analysis of upregulated proteins in UM vitreous detected by two separate proteomics platforms (i.e. multiplex ELISA and LC-MS/MS). Lists of upregulated proteins (compared to controls) at the $P < 0.05$ level were analyzed by Venn diagram analysis. Two proteins were shared between the two platforms: LYVE-1 and plasminogen. (**C**) Venn diagram analysis of upregulated proteins, sorted by PRAME status. Two proteins (angiotensinogen and ENPP2) were commonly detected by LC-MS/MS and multiplex ELISA. (**D**) Venn diagram analysis of upregulated proteins, sorted by GEP class. There were 2 commonly identified proteins (C163A and ANXA5) among GEP class 1 samples and 3 commonly identified proteins (HGFR, ANXA5, and C163A) among GEP class 2 samples.

ANXA5) among GEP class 1 samples and 3 commonly identified proteins (HGFR, ANXA5, and C163A) among GEP class 2 samples (Fig. 3D). Because many of the proteins identified by LC-MS/MS were not included in the multiplex ELISA array, the small degree of overlap between the two platforms is to be expected.

Discussion

Advances in molecular and genetic testing have enhanced the prognostic accuracy and Precision Health management of UM.[12,31,35] Tumor biopsies can be performed either transsclerally or trans-vitreally, with the former method having a risk of extra-scleral extension and the latter having a risk for retinal detachment, hypotony, or vitreous hemorrhage.[36,37] It is also not feasible to repeatedly sample a tumor for increased yield, given the risks of complications. Our studies support the feasibility and utility of obtaining vitreous liquid biopsies in UM to provide additional diagnostic information without violating the retina or disrupting the tumor.

Using shotgun mass-spectrometry (i.e. LC-MS/MS), we identified 69 significantly upregulated proteins in UM vitreous, including proteins that were not previously identified using targeted detection platforms. Among these proteins were LYVE-1, HGFR/c-MET, PYGL, ENPP-2/autotaxin, ANGT, ANXA5, and C163A. Our use of multiple protein detection platforms in the same patient samples strengthens the sensitivity of these candidate biomarkers (i.e. cross-platform validation). LYVE-1 displayed the most statistically significant increase in expression between UM and control vitreous by LC-MS/MS. LYVE-1 is a hyaluronan receptor that is expressed in lymphatic endothelial cells, liver sinusoidal endothelial cells, and macrophages.[38] In addition to binding soluble and immobilized hyaluronan, LYVE-1 may play a role in tumor metastasis by mediating adhesion of leukocytes and cancer cells to endothelial cells.[38] Reduced ENPP-2/autotaxin levels have been previously associated with increased survival in patients with UM.[39] HGFR/c-MET has been demonstrated to play a key role in UM tumorogenesis by influencing cell migration and adhesion, promoting tumor survival (by inducing PI3K/AKT/mTOR signaling), inducing angiogenesis and lymphangiogenesis (through regulation of VEGF and TSP1 expression), and upregulating matrix metalloproteinases.[40–43] HGFR/c-MET expression is frequently observed in metastatic UM and is associated with a poor prognosis and c-MET has been studied as a potential target in the treatment of metastatic UM.[43] In the current study, we detected elevated vitreous HGFR/c-MET expression in patients GEP class 2 tumors by LC-MS/MS and ELISA, further strengthening its potential as an independent prognostic biomarker for UM.

Pathway analysis revealed IGF1 regulatory effectors (e.g. IGFBP6) were highly represented in UM vitreous. Prior studies have suggested that increased IGF1R expression levels in UM primary tumors (by immunoblot and immunohistochemistry analysis) may be associated with increased risk of death from metastatic disease.[34] Cixutuxumab, an IGF1R-specific monoclonal antibody, has shown promise in preclinical studies, its use as a single agent has not been shown to be effective in increasing progression-free survival (PFS) in patients with metastatic UM.[44] Furthermore, tepertumumab, and IGF1 monoclonal antibody has been US Food and Drug

Administration (FDA) approved for the treatment of Graves ophthalmopathy suggesting potential complementary drug therapies that may impact UM metastasis.

Recent single-cell RNA-seq analysis of primary UM tumors and liver metastases identified infiltrating CD8+ T-cells expressing the LAG3 checkpoint marker, potentially explaining why UM has been resistant to checkpoint inhibitors targeting PD-1 and CTLA4.[35] Proteomic analysis may be able to supplement this critical finding by identifying additional markers that could predict the onset of metastatic disease. Additionally, proteomic profiling has the potential to uncover protein signatures which may carry more diagnostic and prognostic value than single proteins alone. This is exemplified in the diagnosis and early detection of ovarian cancer where the use of multiple biomarkers in combination with CA125 outperformed single biomarker assays (with respect to sensitivity and specificity) for early detection of the disease.[45] Moreover, unique patterns of proteins point to biologically plausible mechanisms for tumor proliferation and propagation, and suggest rational approaches for adjuvant therapy, drug repositioning, and metastatic surveillance. This approach may be complementary to primary GEP and PRAME detection from tumor biopsies.

There are few proteomic studies on human ocular melanoma tissues to date and several were limited in that they performed analysis exclusively on enucleated eyes, which biased toward the inclusion of larger tumors.[46–50] Furthermore, few proteomic studies to date have utilized GEP and PRAME classifications in their analysis. In a recent vitreous study of UM, 41 proteins were evaluated in relation to GEP class in a discovery cohort comprising 18 patients with UM.[51] The study identified six differentially expressed proteins (MCP-1, MIP-1a, MIP-1b, IP-10, IL-6, and PDGF-AA) and similarly suggested the prognostic potential of vitreous protein profiling, but was limited in the number of detected DEPs through use of a targeted proteomics platform.[51] Our results from vitreous biopsies are similarly encouraging, and they raise the question of alternative liquid biopsies, including aqueous humor and tears. Another recent liquid biopsy study of UM utilized aqueous humor samples from 90 patients with UM to study the differential expression of 92 pre-selected proteins.[46] This larger cohort size of this study lended to more detailed comparisons of protein expression with regard to patient age, tumor size, ciliary body involvement, AJCC stage, monosomy of chromosome 3, and gain of chromosome 8q.[46] Finally, a recent multiplex proximity extension assay (PEA)-based analysis (measuring 1469 preselected proteins) of aqueous humor samples from 17 patients with UM demonstrated that aqueous protein expression correlated with GEP class.[19] Together, these studies similarly suggest that liquid biopsies could serve as surrogates for direct tumor biopsy and allow for less invasive determination of a low or high-risk lesion which can be potentially repeated as a strategy to guide treatment decisions. Thus, future studies will aim to apply the current findings from our vitreous analysis to other fluids and to compare protein expression among patients with different clinical characteristics (e.g. age, tumor size, AJCC stage, etc.). With aqueous and tear samples, there is no need to use an operating room and incur all the associated costs of equipment and personnel.

There are limitations to the current study. The limited number of samples, high number of measurements, and intra-tumor heterogeneity can introduce bias and false positives. Because of these potential confounders, further verification in a larger cohort is required, and serial samples from the same patients could reveal patient-specific trends. Future studies should involve prospective validation and use liquid biopsies from multiple sites to determine whether changes in protein expression correlate among the vitreous, aqueous, and tears in the same patient.

Liquid biopsies may serve as a less invasive alternative to primary UM tumor biopsies for monitoring disease progression and response to therapy. Our results demonstrate that liquid biopsies can be used to identify proteins of interest which may serve as additional prognostic biomarkers and identify therapeutic targets for UM. The use of multiple protein detection platforms in the same patient samples in the current study allowed for precise characterization of the vitreous proteome and increased the sensitivity of candidate biomarker detection in our pilot cohort. Validation of these proteomic biomarkers in larger patient cohorts and alternative liquid biopsies (i.e. aqueous and tears) should strengthen their value for early prognostic testing. Additionally, these biomarkers could help rationally design future clinical trials for adjuvant therapy, including for previously untreated micro-metastatic UM.

Acknowledgments

The authors thank Jennifer T. Vu, Teja Chemudupati, and Aarushi Kumar for technical assistance.

V.B.M. is supported by National Institutes of Health (NIH) grants (R01EY031952, R01EY031360, and R01EY030151) and The Stanford Center for Optic Disc Drusen. V.B.M. and P.M. are supported by NIH P30EY026877, The Cancer League Research Grant, Research to Prevent Blindness, and The Alan and Irene Adler Ocular Cancer Research Initiative. A.D. is supported the Lion Sight Centre fund and CIHR grant 202104PJT-460696.

Author Contributions: Mahajan and Mruthyunjaya had full access to all the data in the study and take responsibility for the integrity of the data and the accuracy of the data analysis. Study concept and design: P.M. and V.B.M. Acquisition of data: G.V., P.M., and V.B.M.. Analysis and interpretation of data: G.V., J.W., P.M., and V.B.M. Drafting of the manuscript: G.V., P.M., and V.B.M. Critical revision of the manuscript for important intellectual content: G.V., P.M., V.B.M., J.W., and A.D. Statistical analysis: G.V. and V.B.M. Obtained funding: P.M. and V.B.M. Administrative, technical, and material support: P.M. and VBM. Study supervision: V.B.M. and P.M.

Role of the Sponsor: The funding organizations had no role in design and conduct of the study; collection, management, analysis, and interpretation of the data; preparation, review, or approval of the manuscript; and decision to submit the manuscript for publication.

Disclosure: **G. Velez**, None; **J. Wolf**, None; **A. Dufour**, None; **P. Mruthyunjaya**, None; **V.B. Mahajan**, None

References

1. Singh AD, Turell ME, Topham AK. Uveal melanoma: trends in incidence, treatment, and survival. *Ophthalmology*. 2011;118:1881–1885.
2. Singh AD, Bergman L, Seregard S. Uveal melanoma: epidemiologic aspects. *Ophthalmol Clin North Am*. 2005;18:75–84, viii.

3. Bell DJ, Wilson MW. Choroidal melanoma: natural history and management options. *Cancer Control*. 2004;11:296–303.
4. Eskelin S, Pyrhonen S, Summanen P, Hahka-Kemppinen M, Kivela T. Tumor doubling times in metastatic malignant melanoma of the uvea: tumor progression before and after treatment. *Ophthalmology*. 2000;107:1443–1449.
5. Carvajal RD, Schwartz GK, Tezel T, Marr B, Francis JH, Nathan PD. Metastatic disease from uveal melanoma: treatment options and future prospects. *Br J Ophthalmol*. 2017;101:38–44.
6. Barker CA, Salama AK. New NCCN guidelines for uveal melanoma and treatment of recurrent or progressive distant metastatic melanoma. *J Natl Compr Canc Netw*. 2018;16:646–650.
7. McLean IW, Foster WD, Zimmerman LE, Gamel JW. Modifications of callender's classification of uveal melanoma at the armed forces institute of pathology. *Am J Ophthalmol*. 2018;195:lvi–lx.
8. Kivelä T, Simpson RE, Grossniklaus HE. Uveal melanoma. In: Amin MB, Edge S, Greene F, et al., eds. *AJCC Cancer Staging Manual*. New York, NY: Springer International Publishing; 2016:805–817.
9. Seider MI, Mruthyunjaya P. Molecular prognostics for uveal melanoma. *Retina*. 2018;38:211–219.
10. Onken MD, Worley LA, Char DH, et al. Collaborative Ocular Oncology Group report number 1: prospective validation of a multi-gene prognostic assay in uveal melanoma. *Ophthalmology*. 2012;119:1596–1603.
11. Landreville S, Agapova OA, Harbour JW. Emerging insights into the molecular pathogenesis of uveal melanoma. *Future Oncol*. 2008;4:629–636.
12. Cai L, Paez-Escamilla M, Walter SD, et al. Gene expression profiling and PRAME status versus tumor-node-metastasis staging for prognostication in uveal melanoma. *Am J Ophthalmol*. 2018;195:154–160.
13. Raja V, Russo A, Coupland S, Groenewald C, Damato B. Extraocular seeding of choroidal melanoma after a transretinal biopsy with a 25-gauge vitrector. *Retin Cases Brief Rep*. 2011;5:194–196.
14. Schefler AC, Gologorsky D, Marr BP, Shields CL, Zeolite I, Abramson DH. Extraocular extension of uveal melanoma after fine-needle aspiration, vitrectomy, and open biopsy. *JAMA Ophthalmol*. 2013;131:1220–1224.
15. Mashayekhi A, Lim RP, Shields CL, Eagle RC, Jr., Shields JA. Extraocular extension of ciliochoroidal melanoma after transscleral fine-needle aspiration biopsy. *Retin Cases Brief Rep*. 2016;10:289–292.
16. Finn AP, Materin MA, Mruthyunjaya P. Choroidal tumor biopsy: a review of the current state and a glance into future techniques. *Retina*. 2018;38(Suppl 1):S79–S87.
17. Velez G, Tang PH, Cabral T, et al. Personalized proteomics for precision health: identifying biomarkers of vitreoretinal disease. *Transl Vis Sci Technol*. 2018;7:12.
18. Li HT, Xu L, Weisenberger DJ, et al. Characterizing DNA methylation signatures of retinoblastoma using aqueous humor liquid biopsy. *Nat Commun*. 2022;13:5523.
19. Peng CC, Sirivolu S, Pike S, et al. Diagnostic aqueous humor proteome predicts metastatic potential in uveal melanoma. *Int J Mol Sci*. 2023;24(7):6825.
20. Skeie JM, Roybal CN, Mahajan VB. Proteomic insight into the molecular function of the vitreous. *PLoS One*. 2015;10:e0127567.
21. Wert KJ, Velez G, Kanchustambham VL, et al. Metabolite therapy guided by liquid biopsy proteomics delays retinal neurodegeneration. *EBioMedicine*. 2020;52:102636.
22. Velez G, Nguyen HV, Chemudupati T, et al. Liquid biopsy proteomics of uveal melanoma reveals biomarkers associated with metastatic risk. *Mol Cancer*. 2021;20:39.
23. Grewal DS, Cummings TJ, Mruthyunjaya P. Outcomes of 27-gauge vitrectomy-assisted choroidal and subretinal biopsy. *Ophthalmic Surg Lasers Imaging Retina*. 2017;48:406–415.
24. Velez G, Roybal CN, Colgan D, Tsang SH, Bassuk AG, Mahajan VB. Precision medicine: personalized proteomics for the diagnosis and treatment of idiopathic inflammatory disease. *JAMA Ophthalmol*. 2016;134:444–448.
25. Harbour JW, Paez-Escamilla M, Cai L, Walter SD, Augsburger JJ, Correa ZM. Are risk factors for growth of choroidal nevi associated with malignant transformation? Assessment with a validated genomic biomarker. *Am J Ophthalmol*. 2019;197:168–179.
26. Gezgin G, Luk SJ, Cao J, et al. PRAME as a potential target for immunotherapy in metastatic uveal melanoma. *JAMA Ophthalmol*. 2017;135:541–549.
27. Raudvere U, Kolberg L, Kuzmin I, et al. g:Profiler: a web server for functional enrichment analysis and conversions of gene lists (2019 update). *Nucleic Acids Res*. 2019;47:W191–W198.
28. Fabregat A, Sidiropoulos K, Viteri G, et al. Reactome pathway analysis: a high-performance in-memory approach. *BMC Bioinformatics*. 2017;18:142.
29. Force AOOT. International validation of the American Joint Committee on Cancer's 7th Edition Classification of Uveal Melanoma. *JAMA Ophthalmol*. 2015;133:376–383.
30. Mellen PL, Morton SJ, Shields CL. American Joint Committee on cancer staging of uveal melanoma. *Oman J Ophthalmol*. 2013;6:116–118.
31. Field MG, Decatur CL, Kurtenbach S, et al. PRAME as an independent biomarker for metastasis in uveal melanoma. *Clin Cancer Res*. 2016;22:1234–1242.
32. Onken MD, Worley LA, Tuscan MD, Harbour JW. An accurate, clinically feasible multi-gene expression assay for predicting metastasis in uveal melanoma. *J Mol Diagn*. 2010;12:461–468.
33. Papastefanou VP, Islam S, Szyszko T, Grantham M, Sagoo MS, Cohen VM. Metabolic activity of primary uveal melanoma on PET/CT scan and its relationship with monosomy 3 and other prognostic factors. *Br J Ophthalmol*. 2014;98:1659–1665.
34. All-Ericsson C, Girnita L, Seregard S, Bartolazzi A, Jager MJ, Larsson O. Insulin-like growth factor-1 receptor in uveal melanoma: a predictor for metastatic disease and a potential therapeutic target. *Invest Ophthalmol Vis Sci*. 2002;43:1–8.
35. Durante MA, Rodriguez DA, Kurtenbach S, et al. Single-cell analysis reveals new evolutionary complexity in uveal melanoma. *Nat Commun*. 2020;11:496.
36. Angi M, Kalirai H, Taktak A, et al. Prognostic biopsy of choroidal melanoma: an optimised surgical and laboratory approach. *Br J Ophthalmol*. 2017;101:1143–1146.
37. Singh AD, Medina CA, Singh N, Aronow ME, Biscotti CV, Triozzi PL. Fine-needle aspiration biopsy of uveal melanoma: outcomes and complications. *Br J Ophthalmol*. 2016;100:456–462.
38. Karinen S, Hujanen R, Salo T, Salem A. The prognostic influence of lymphatic endothelium-specific hyaluronan receptor 1 in cancer: a systematic review. *Cancer Sci*. 2022;113:17–27.
39. Singh AD, Sisley K, Xu Y, et al. Reduced expression of autotaxin predicts survival in uveal melanoma. *Br J Ophthalmol*. 2007;91:1385–1392.
40. Ye M, Hu D, Tu L, et al. Involvement of PI3K/Akt signaling pathway in hepatocyte growth factor-induced migration of uveal melanoma cells. *Invest Ophthalmol Vis Sci*. 2008;49:497–504.
41. Zhang YW, Su Y, Volpert OV, Vande Woude GF. Hepatocyte growth factor/scatter factor mediates angiogenesis through

Investigative Ophthalmology & Visual Science

positive VEGF and negative thrombospondin 1 regulation. *Proc Natl Acad Sci USA*. 2003;100:12718–12723.

42. Koh SA, Lee KH. HGF mediated upregulation of lipocalin 2 regulates MMP9 through nuclear factor-kappaB activation. *Oncol Rep*. 2015;34:2179–2187.
43. Tanaka R, Terai M, Londin E, Sato T. The role of HGF/MET signaling in metastatic uveal melanoma. *Cancers (Basel)*. 2021;13(21):5457.
44. Mattei J, Ballhausen A, Bassett R, et al. A phase II study of the insulin-like growth factor type I receptor inhibitor IMC-A12 in patients with metastatic uveal melanoma. *Melanoma Res*. 2020;30:574–579.
45. Muinao T, Deka Boruah HP, Pal M. Multi-biomarker panel signature as the key to diagnosis of ovarian cancer. *Heliyon*. 2019;5:e02826.
46. Wierenga APA, Cao J, Mouthaan H, et al. Aqueous humor biomarkers identify three prognostic groups in uveal melanoma. *Invest Ophthalmol Vis Sci*. 2019;60:4740–4747.
47. Shi XY, Li Q, Wei WB, Tao LM. Peptidome profiling of human serum of uveal melanoma patients based on magnetic bead fractionation and mass spectrometry. *Int J Ophthalmol*. 2017;10:939–947.
48. Linge A, Kennedy S, O'Flynn D, et al. Differential expression of fourteen proteins between uveal melanoma from patients who subsequently developed distant metastases versus those who did Not. *Invest Ophthalmol Vis Sci*. 2012;53:4634–4643.
49. Song J, Merbs SL, Sokoll LJ, Chan DW, Zhang Z. A multiplex immunoassay of serum biomarkers for the detection of uveal melanoma. *Clin Proteomics*. 2019;16:10.
50. Crabb JW, Hu B, Crabb JS, et al. iTRAQ quantitative proteomic comparison of metastatic and non-metastatic uveal melanoma tumors. *PLoS One*. 2015;10:e0135543.
51. Demirci H, Tang L, Demirci FY, Ozgonul C, Weber S, Sundstrom J. Investigating vitreous cytokines in choroidal melanoma. *Cancers (Basel)*. 2023;15(14):3701.

Investigative Ophthalmology & Visual Science